S22-20

50407

125895

10p

LABORATORY INSTRUMENTATION AND TECHNIQUES FOR CHARACTERIZING MULT-JUNCTION SOLAR CELLS FOR SPACE APPLICATIONS*

James R. Woodyard
Wayne State University
Detroit, Michigan 48202

ABSTRACT

An integrated system is described which consists of a spectral radiometer and dual-source solar simulator, and personal computer based current-voltage and quantum efficiency equipment. The spectral radiometer is calibrated using a tungsten-halogen standard lamp with a calibration based on NIST scales. The quantum efficiency apparatus includes a photodiode calibrated using NIST scales and a monochromatic probe beam. The apparatus is used to measure the dependence of the absolute external quantum efficiency of solar cells at various forward-bias voltages including the maximum-power point under AM0 light bias. Quantum efficiencies of multi-junction cells were measured with both spectral-light bias and AM0 light bias. Measured spectral irradiances of the dual-source simulator were convoluted with cell quantum efficiencies to calculate cell currents as function of voltage. The calculated currents agree with measured currents at the 1% level.

INTRODUCTION

Multi-junction solar cells are attractive for space applications because they can be designed to convert a larger fraction of AM0 into electrical power than single-junction cells. The performance of multi-junction cells is much more sensitive to the spectral irradiance of the illuminating source than single-junction cells. The design of high efficiency multi-junction cells for space applications requires matching the optoelectronic properties of the junctions to AM0 spectral irradiance. Unlike single-junction cells, it is not possible to determine the quantum efficiency of multi-junction cells using only a monochromatic probe beam. It is necessary to use a light bias because of the series nature of the cell structure. Burdick and Glatfelter (1) reported a measurement technique for multi-junction cells which employs a spectral light-bias technique. While the method is useful for understanding and improving multi-junction solar cells, it does not yield the absolute quantum efficiency under AM0 light-bias. Because of the non-linear nature of multi-junction cells, current-voltage characteristics under AM0 conditions cannot be calculated from measurements under non-AM0 conditions using spectral-correction methods.

The goal of the research is to develop a solar simulator which approximates AM0 spectral irradiance, and laboratory instrumentation and techniques, for use in measuring the quantum efficiency and I-V characteristics of multi-junction solar cells under AM0 power-generating conditions. An integrated system is described which consists of a spectral radiometer and dual-source solar simulator, and personal computer based current-voltage and quantum efficiency equipment. The spectral radiometer is calibrated using a tungsten-halogen standard lamp which has a calibration traceable to National Institute of Science and Technology (NIST) scales. The calibrated spectral radiometer is used to measure the spectral irradiance of the light-bias beam and obtain an integral fit of it in two spectral regions to the World Radiation Laboratory (WRL) AM0 spectral irradiance data. The solar simulator produces a light-bias beam which is used for current-voltage and external absolute quantum efficiency measurements. The quantum efficiency apparatus includes a photodiode calibrated using NIST scales and a monochromatic probe beam. The apparatus is used to measure the absolute external quantum efficiency of triple-junction solar cells at various forward-bias voltages under both spectral-light and AM0 light-bias conditions.

SOLAR SIMULATOR DEVELOPMENT

The spectral irradiance of the solar simulator plays an important role in the characterization of multi-junction solar cells. Characterization techniques such as light I-V and light-biased quantum efficiency measurements require

matching the solar simulator spectral irradiance as close as possible to the AM0 spectrum in order to predict the performance of cells in a space environment with AM0 illuminance.

The spectral irradiance of the solar simulator used in this work was measured with a spectral radiometer constructed and calibrated in our laboratory. The spectral radiometer employs an integrating sphere, order-sorting filters, single-stage monochromator and detector; the detector is a silicon photodiode and temperature stabilized. The instrument is computer interfaced for control purposes, and data acquisition, display and analyses. The spectral radiometer was calibrated with a type FEL 1000 W quartz tungsten-halogen standard lamp traceable to NIST scales; calibrations were carried out using the procedure specified in NBS Special Publication 250-20. The accuracy of measurements in the 350 to 900 nm range is believed to be better than 4%; the precision of consecutive spectral scans is better than 1%.

A model SS1000 solar simulator manufactured by Optical Radiation Corporation (ORC) was used in this work. The light source in the simulator is a xenon high-pressure discharge lamp. The spectral irradiance of the solar simulator, as delivered by ORC, is shown in Figure 1 by the filled circles. The spectral irradiance of the WRL AM0 solar spectrum is shown for comparison purposes in the figure by the solid line. The spectral irradiance of the simulator differs from AM0 in a major way in the 300 to 370 nm and 650 to 1000 nm wavelength ranges. Above 800 nm the spectral irradiance of the solar simulator is dominated by xenon lines. The differences in spectral irradiances of the ORC solar simulator when compared to AM0, while generally not important in characterizing single-junction solar cells, can introduce major errors in light I-V and quantum efficiency measurements of multi-junction cells.

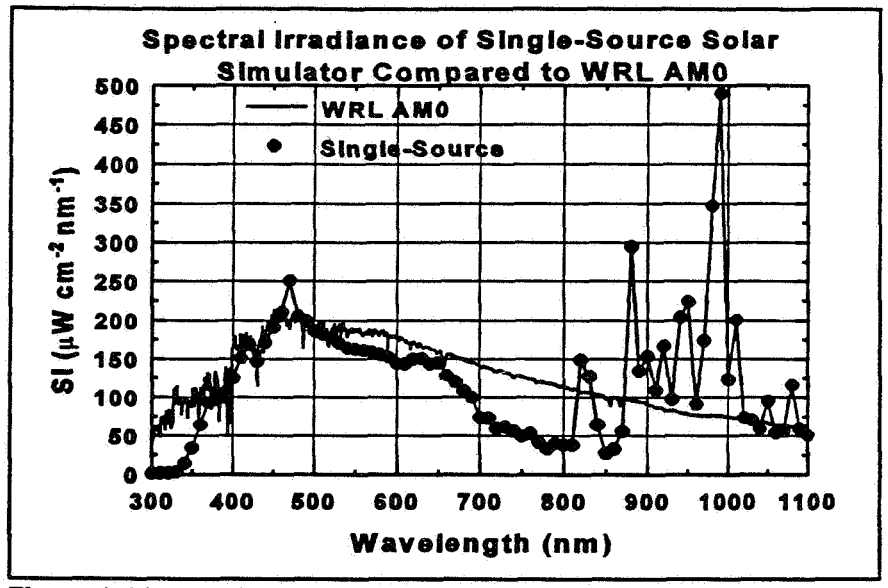

Figure 1: Measured spectral irradiance of single-source solar simulator compared with World Radiation Laboratory AM0 spectral irradiance.

The solar simulator was modified to produce a spectral irradiance in closer agreement with the spectral irradiance of the AM0 solar spectrum using a design reported by Bennett and Podlesny (2). In order to obtain a better match with the AM0 spectral irradiance at wavelengths above 700 nm, a 600 W tungsten-halogen lamp and cold mirror were added to the solar simulator. A diagram illustrating the optics of the modified simulator is show in Figure 2. The design includes two elliptical mirrors and a flat cold mirror to focus illumination from the tungsten-halogen and xenon lamps on an optical integrator; the design produces a horizontal light beam which is compatible with the horizontal optics of the spectral radiometer and quantum efficiency apparatus. The cold mirror was custom fabricated to transmit wavelengths greater than 750 nm and reflect shorter wavelengths. The original folding mirror in the simulator was replaced with the cold mirror; it is mounted at forty-five degrees with respect to both the xenon and tungsten-halogen lamps. The cold mirror serves two purposes. It trans-

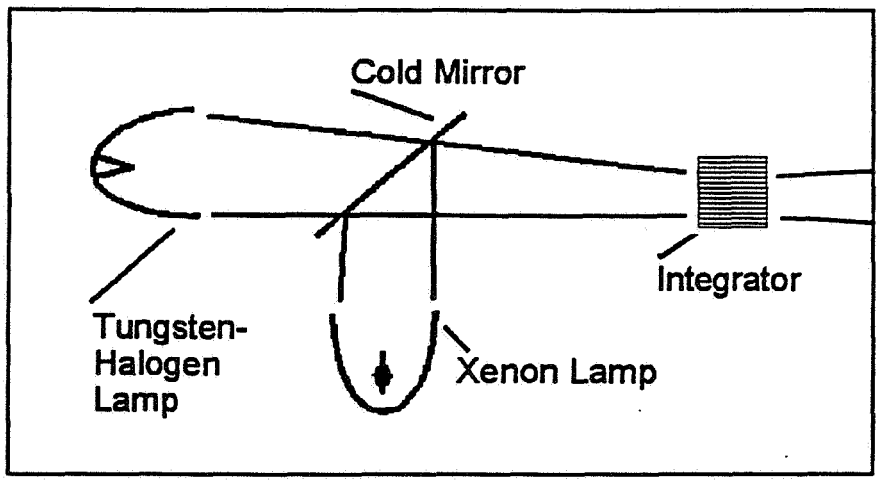

Figure 2: Optics of Dual-Source Simulator

mits the xenon spectrum at wavelengths greater than 750 nm and reflects wavelengths less than 750 nm. The effec of the mirror on the spectral irradiance of the xenon lamp is to attenuate the xenon lines shown in Figure 1. The mirrc transmits the spectral irradiance of the tungsten-halogen lamp with wavelengths greater than 750 nm while reflectin wavelengths less than 750 nm.

The optics of the solar simulator, as delivered by ORC, incorporated a second folding mirror, Vicor beam splitte and Pyrex collimating lens. The Vicor beam splitter was used to produce an optical signal for the feed-back circu which stabilizes the xenon lamp current. The folding mirror and collimating lens produce a vertical beam focussed o a horizontal work surface. The folding mirror and lens were removed to produce a horizontal light beam. The Vicc beam splitter was replaced with a high-quality quartz beam splitter. The modification in the optics also increased th UV throughput of the simulator. Additional air cooling capacity was added in order to dissipate the power produced b the tungsten-halogen lamp. The electronics supplied by ORC with the simulator were used to power and control th xenon lamp. A D.C. power supply regulated at the 0.01 % level was added to the system for powering the tungster halogen lamp. The stability of the dual-source light beam intensity is at the 0.1 % level.

The spectral irradiance of the dual-source solar simulator was fit to the WRL AM0 spectrum by integrating an comparing the two spectral irradiances in two regions. The simulator and WRL spectral irradiances were integrate in two regions and compared. One region employed wavelength limits of 350 and 750 nm; the other region had limit of 750 and 900 nm. The limits of 350 and 900 nm were selected because the quantum efficiency of the triple-junctio solar cells investigated in this work is negligible outside this wavelength range. The wavelength limit of 750 was selecte because it is the bandpass of the cold mirror. Selection of the two regions in this manner made it possible to obtai integrated spectral irradiance fits in each region almost independently of each other by adjusting the current in th corresponding lamp; most of the spectral irradiance in the 350-750 nm range is due to the xenon lamp while th tungsten-halogen lamp produces most of the spectral irradiance in the 750-900 nm range.

The fit of the solar simulator spectral irradiance to the WRL AM0 spectrum was carried out using a procedur which included calibrating the spectral radiometer; adjusting the currents in the xenon and tungsten lamps; measurin the simulator spectral irradiance; integrating the measured and WRL AM0 spectral irradiances in the 350 to 750 nm and 750 to 900 nm ranges; calculating the percentage error in the integrated measured and WRL AM0 spectral irradiances in the two wavelength regions; and repeating the process until the error in each of regions was less than 1%. The spectral irradiance of the dual-source simulator compared to the WRL AM0 spectrum is shown in Figure 3 by the filled circles. Comparison of the spectral irradiances in Figures 1 and 3 shows the dual-source solar simulator produces a spectral irradiance which is in significantly better agreement with the WRL AM0 spectrum. The percentage difference between the integrated spectral irradiance of dual-source simulator compared to WRL AM0 in Figure 3 is +0.06% in the 350 to 750 nm wavelength range and -0.9% in the 750 to 900 nm range.

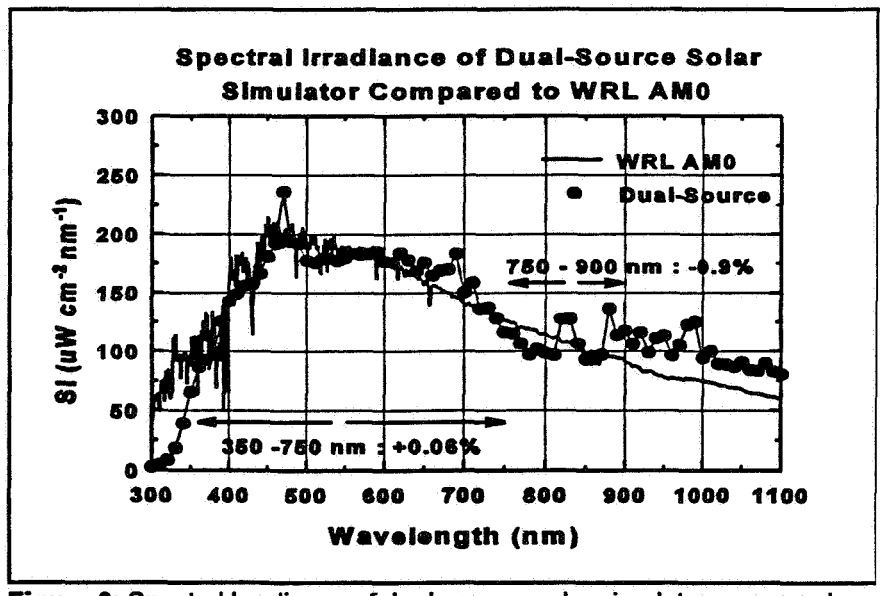

Figure 3: Spectral Irradiance of dual-source solar simulator compared with World Radiation Laboratory AM0 spectral irradiance.

QUANTUM EFFICIENCY SYSTEM DESCRIPTION

The quantum efficiency (QE) system was designed and constructed to carry out measurements und three conditions: dark, spectral-light bias and AM0 light bias. A second personal computer is used to control the Q system, as well as data acquisition, display and analyses. The design permits quantum efficiency measurements wi an accuracy better than 2% over the 400 to 1000 nm wavelength range. The probe beam intensity and calibrate

detector response result in reductions in accuracy outside this wavelength range. The major components of the system include two computer-interfaced Scientific Measurement System, Inc. MonoSpec 27 monochromators; two computer-interfaced motorized filter wheels with filters for order sorting and spectral-light bias; UV-grade fused silica lenses and beam splitter; two magnesium fluoride coated Al mirrors; computer interfaced Stanford Research Systems model SR830 DSP lock-in amplifier and chopper; 60 watt quartz-tungsten-halogen (QTH) lamp; and a computer-interfaced Hewlett-Packard model 6038A power supply for the QTH lamp.

The two monochromators were mounted in tandem and used with the QTH lamp to produce a monochromatic probe beam for QE measurements of solar cells. Two monochromators are employed to reduce the stray-light level in the probe beam. Each monochromator has a ruled 1200 grooves/mm grating blazed at 500. The subtractive mode is used for the physical configuration of the monochromators along with 4 mm slit widths to optimize light throughput. The measured resolution of the two monochromators is 20 nm. The monochromators are capable of higher resolution at the expense of probe beam intensity. The monochromator containing the entrance slit and located next to the input optics is referred to as monochromator #1 in the following discussion; the other monochromator contains the exit slit and is referred to as monochromator #2.

Optical components located in front of the entrance silt of monochromator #1 serve to focus an A.C. light beam on the entrance slit and provide order-sorting capability. The optics include a QTH lamp, collimating lens, beam chopper and filter wheel. The beam chopper and filter wheel are mounted next to the entrance slit of the first monochromator. The beam chopper is used in conjunction with the lock-in amplifier to detect the response of the test solar cell to the monochromatic A.C. probe beam. The filter wheel contains four long pass filters. The filters provide order-sorting of the light-beams passing through the monochromators. The filters serve to reject the nth order beams of wavelength λ/n in the QE probe; the higher order beams can introduce large errors in QE measurements.

The optical components at the exit slit of monochromator #2 produce two light beams from the A.C. monochromatic probe beam which passes through the exit slit. The beams are used to measure the absolute external QE of a test solar cell. The configuration of the optical components is shown in Figure 4. The components include a beam splitter, two mirrors, lens, calibrated silicon photodiode, test-cell holder and filter wheel, and miscellaneous optical rails and holders. The components are enclosed in a black light-tight aluminum box. The monochromatic A.C. probe beam emanating from the exit slit of monochromator #2 is split into two separate light beams by the beam splitter. The light beam reflected from the beam splitter is focussed on the calibrated detector by the lens; the detector is a calibrated silicon photodiode and serves as the reference detector for the QE measurements. The photodiode calibration is traceable to NIST scales and permits determining the absolute number of photons incident on the test cell. The second light beam transmits the beam splitter and is incident on the flat mirror; it is reflected onto the concave mirror which focusses the beam on the test cell. The optics do not permit measurement of the reflected light from the test cell. The QE values measured by the system and reported in this paper are absolute external quantum efficiencies.

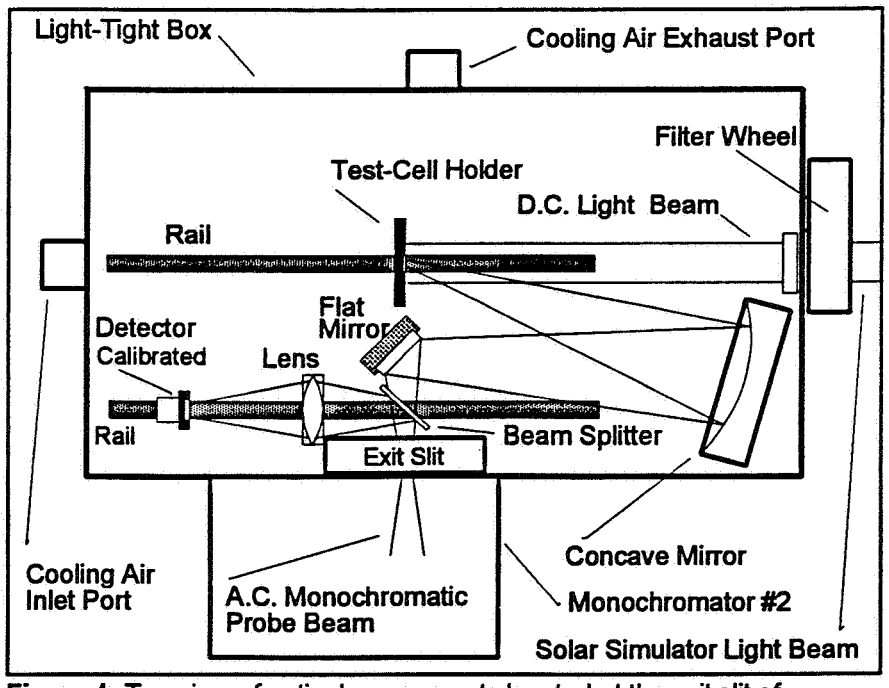

Figure 4: Top view of optical components located at the exit slit of monochromator #2.

A D.C. light beam originating from the solar simulator and passing through the filter wheel shown in Figure 4 is incident on the test cell; it is coincident with the optical axis defined by the test cell and filter wheel. The spectral content of the light beam is determined by the filter wheel. Three positions on the filter wheel are used to hold filters which pass spectra for measuring QE of triple-junction cells under spectral-light bias conditions (1); each filter passes

a portion of the simulator spectrum for "turning-on" two of the three junctions of a test cell. One position on the filter wheel is open and used for AM0 light-bias measurements; another position contains a black aluminum disk and is used for measuring QE under dark conditions.

Temperature control of solar cells during light-bias measurements is accomplished by directing room temperature air on the back of the cell mounted in the test-cell holder. Figure 4 shows the cooling air inlet port which is mounted opposite the test-cell holder. Air is exhausted through the cooling air exhaust port which is baffled to prevent ambient light from entering the light-tight box. The air flow is set to insure the active junction of the test solar cell is maintained at room temperature; the junction temperature is monitored by measuring the open circuit voltage of the test cell. Temperature probes are included in the system to monitor the ambient air temperature in the light-tight box and the temperature of the test-cell holder.

The system was designed to minimize electrical noise. Electrical connection of the test and reference cells to a multiplexer and lock-in-amplifier are made with BNC cables and connectors. Ground loops are minimized through the use of a single common ground for all the electrical components; all electrical components are also electrostatically shielded. The background current levels are less than 1E-12 A and the A.C. monochromatic probe currents of the order of 1E-6 A. The wavelength is scanned by stepping both of the monochromators in 20 nm intervals, and measuring and logging ten values of the current at each wavelength. The standard deviation of the ten current values is typically of the order of 1E-3 of the average value of the measured current. The calibrated detector and test cell currents are measured sequentially at each wavelength using a multiplexing circuit and lock-in amplifier.

Calibration of the QE system is accomplished following alignment of the optical components and carrying out two scans. One scan is carried out with the calibrated detector in the position shown in Figure 4; a second scan is done with the calibrated detector positioned in place of the test-cell holder. Computer software is used to calculate a calibration vector which is used in subsequent scans to determine the absolute external QE of solar cells mounted in the test-cell holder. The calibration vectors are saved on the hard drive and used to determine the long-term stability of the system. Following a wavelength scan, absolute external QE values are displayed on the computer monitor in graphical form and in tabular form on the printer. The tabular data are also saved on the computer hard drive for archival purposes and subsequent analyses. Computer control of the filter wheels, monochromators, QTH lamp power supply, and lock-in amplifier makes it possible to measure QE over a selected wavelength range in about twenty minutes. The stability of the system for successive scans is at the 0.1% level.

SINGLE-JUNCTION QE RESULTS

The instrumentation was used to measure the absolute external QE of a single-junction a-Si:H alloy solar cell with a superstrate structure (3). The results of the measurements for the cell without light bias at 24 °C under short-circuit conditions are shown in Figure 5 by the open-square symbols. The maximum value in QE is 0.81 and occurs at 590 nm. QE decreases below 400 nm because of absorption in the glass superstrate and top p-doped layer. The reduction in QE above 700 nm is due to the band gap of the intrinsic layer. The details of QE in the 400 to 700 nm range reflect the roles of the doped layers, intrinsic layer thickness and carrier transport. QE was measured at 24 °C using the AM0 light bias shown in Figure 3; the results are shown in Figure 5 by the open triangular symbols. The effect of AM0 light bias on QE is not discernible on the graph. The measurements show that changes in the occupancy of the sub-band-gap states resulting from high carrier injection levels do not

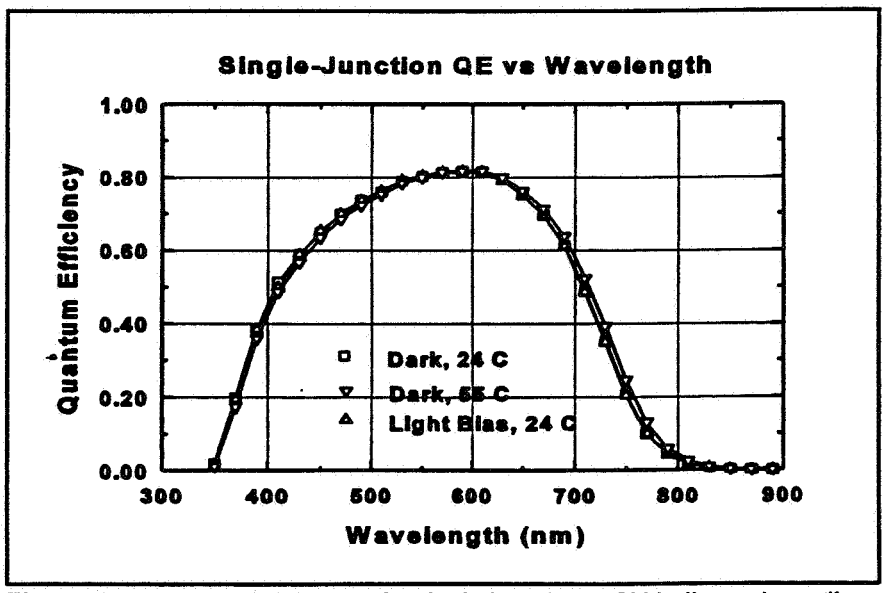

Figure 5: Quantum Efficiency of a single junction a-Si:H alloy solar cell under dark and light-bias conditions at 24 °C, and under dark conditions at 55 °C.

have a major effect on carrier transport and collection in single-junction a-Si:H alloy solar cells. The light-tight box shown in Figure 4 was heated to 55 °C and QE measured under dark conditions. The results of the measurements are shown by the inverted triangular symbols in Figure 5. QE differences of the order of a few percent are discernible and may be attributed to the temperature coefficients of both the test cell and calibrated detector. The 55 °C measurements show the techniques employed are not critically sensitive to room temperature variations of the order of a few degrees.

The effect of forward-bias voltage on QE for a single-junction a-Si:H alloy solar cell was investigated under light-bias conditions at 24 °C. The voltage was stepped in increments of 0.1 V from 0.0 to 0.8 V. The results of the measurements are shown in Figure 6. The measurements show QE is insensitive to forward bias from 0.0 to 0.5 V. The peak value in QE is 0.8 and occurs at 580 nm. At a forward bias of 0.6 V, approximately the maximum-power point, QE begins to decrease and the peak value shifts to lower wavelengths. Significant decreases occur in QE as the forward bias is increased and approaches the open-circuit voltage. At 0.8 V, the peak in QE is 520 nm and the value is 0.08. An interpretation of the wavelength shift in the peak of QE shown in Figure 6 is as the forward bias voltage is increased, the trapped charge in the intrinsic layer plays an increasing important role in skewing the electric field distribution towards the front of the cell; this in turn shifts the peak in QE to a lower wavelength, and influences carrier transport and decreases carrier collection.

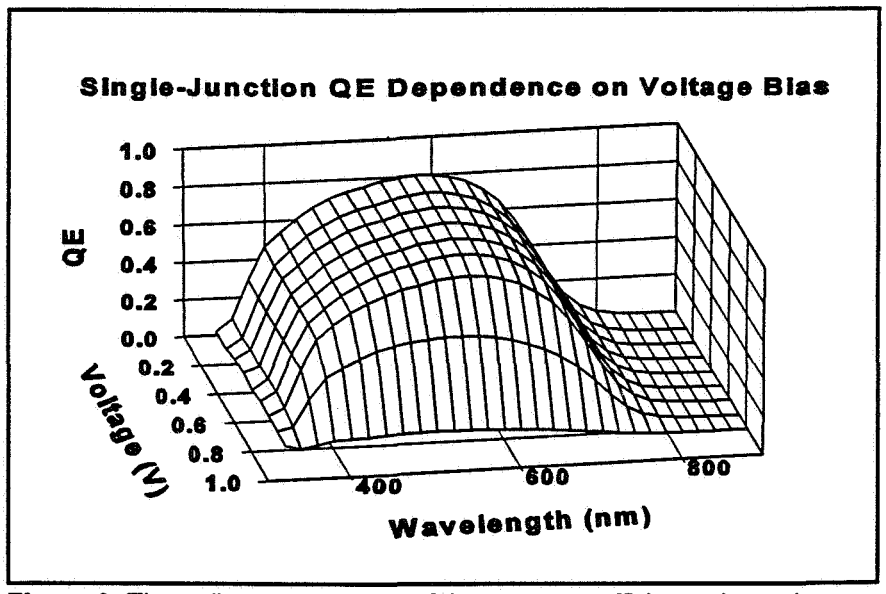

Figure 6: Three dimensional view of the quantum efficiency dependence on forward-bias voltage for a single-junction a-Si:H alloy solar cell.

The instrumentation and measurement methods were evaluated by comparing the short-circuit current measured under AM0 light bias, Isc (meas), with a calculated short-circuit current, Isc (calc). The value of the calculated short-circuit current was obtained by convoluting the measured quantum efficiency values, QE (λ_i), shown in Figure 5 with the measured spectral irradiance values, SI(λ_i), shown in Figure 3. The convolution was carried out over the 350 to 900 nm wavelength range. The calculated short-circuit current was obtained using the expression:

Equation 1

$$Isc(calc) = \frac{A}{1239} \sum_i QE(\lambda_i) \times SI(\lambda_i) \times \lambda_i \times \Delta\lambda \quad [\frac{Coulombs}{Joules \times nm}]$$

where λ_i is the wavelength, $\Delta\lambda$ the monochromator step width and A the cell area. The results of the convolution are shown in Table I. The agreement of Isc (meas) with Isc(calc) is better than 1%. Isc (meas) was measured with a Keithley model 236 source measurement unit recently calibrated with NIST scales referenced to NIST publications #252194 and #251357; Isc (calc) was calculated using measured QE(λ_i) and SI(λ_i) values traceable to NIST scales, as indicated in the preceding section. The agreement between Isc (calc) and Isc (meas) is believed to result from using good measurement techniques and instrumentation calibrated with scales traceable to NIST. The measurements characterize the behavior of a single-junction a-Si:H cell under forward and light bias. They also demonstrate the validity of the measurement techniques for characterizing single-junction solar cells. These observations alos prove useful in understanding the behavior of triple- junction solar cells under various biasing conditions.

Table I

Cell	Isc(meas) (ma)	Isc(calc) (mA)	ΔIsc/ Isc (%)
X302	6.315	6.353	0.6%

SPECTRAL-BIAS TRIPLE-JUNCTION QUANTUM EFFICIENCY RESULTS

QE measurements of triple-junction a-Si:H cells under short-circuit conditions were carried out using th spectral light-bias technique (1). The structure of the triple-junction cells has been previously discussed (3). The light bias technique is based on selectively injecting carriers in cell junctions, and "turning-off" and "turning-on" junctions A junction is referred to as "turned-off" when there is relatively little optical injection of carriers in the junction; it i "turned-on" when there is a relatively large optical injection of carriers. When one junction is "turned-off", and the othe two junctions are "turned-on", the "turned-off" junction limits the current in the cell. QE of a junction limiting the ce current can be determined using an A.C. monochromatic light beam, referred to as the probe beam. The carrier injected by the probe beam in the "turned-off" junction increase the photoconductivity and produce an A.C. current whic characterizes QE of the junction under the conditions of the measurement. The injection of carriers in the junctions i determined by the spectral irradiance of the D.C. light beam and the optoelectronic properties of each of the three junctions. The spectral irradiance of the D.C. light beam used in the spectral light-bias technique is varied to selectively "turn-on" two of the three junctions in the triple-junction solar cell. The filter wheel contains three filters; each filter has a spectral transmission which filters the AM0 solar simulator beam to produce a spectral irradiance which "turns-on" two of the three junctions. The first filter "turns-on" the middle and bottom junctions, the second filter "turns-on" the top and bottom filters, and the third filter "turns-on" the top and middle junctions. Thus the first filter makes it possible to measure QE of the top junction, the second filter the QE of the middle junction, and the third filter the QE of the third junction.

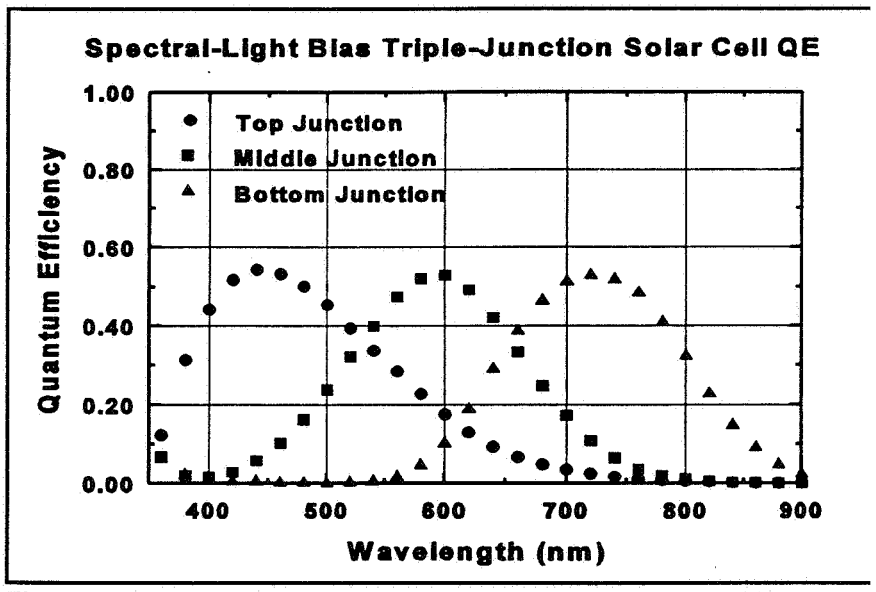

Figure 7: Spectral light-bias quantum efficiencies of the top, middle and bottom junctions for an a-Si:H triple-junction solar cell.

The quantum efficiencies measured with the spectral-light bias technique for the top, middle and bottom junctions of an a-Si:H alloy triple-junction solar cell are shown Figure 7; the values were measured at 24 °C. the top junction is represented by the curve with the closed circles. The peak in QE of the top junction is about 0.54 at 440 nm. QE of the middle junction is shown by the closed squares; it peaks at 600 nm with a value of about 0.53. QE of the third junction is represented by the closed triangles and peaks at 720 nm with a value of about 0.53.

The relative intensity of the A.C. probe and D.C. spectral light-bias was investigated and the results are shown in Figure 8. The intensity of the probe beam is important in obtaining reliable QE values. The probe beam intensity must be much less the intensities of the three D.C. spectral light-bias beams.

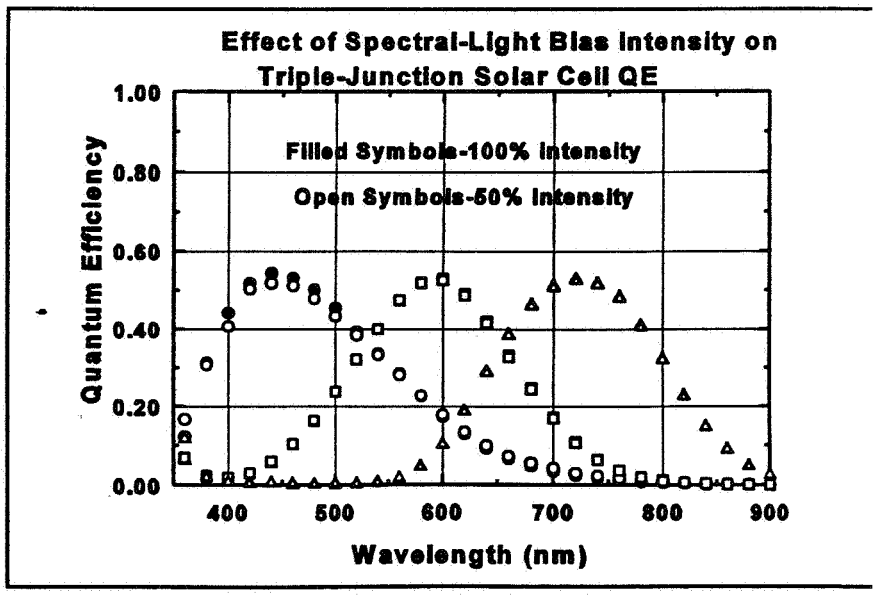

Figure 8: Effect of spectra-light bias intensity on QE for an a-Si:H alloy triple-junction solar cell.

The role of the relative beam intensities was evaluated by measuring QE with an attenuated probe beam and comparing it with QE values obtained with an unattenuated probe beam. The results of measurements with a 50% probe beam attenuation are shown in Figure 8. The symbols used to represent the various junctions are the same as Figure 7. Filled symbols represent QE measurements with the unattenuated probe beam; the QE values measured with the unattenuated beam are referred to as 100% intensity in Figure 8. The open symbols in the figure are plotted over the closed symbols and correspond to QE values measured with the probe beam attenuated 50%. Figure 8 shows QE of the middle and bottom junctions is not influenced by the probe beam intensity; the top junction shows a reduction in measured QE values of the order of a few percent when the probe beam intensity is attenuated by 50%. Hence it may be concluded the QE values obtained with the spectral light-bias technique are not significantly influenced by the probe beam intensities used in these measurements.

The measurements on the triple-junction solar cells show the top junction is effective in absorbing the shorter wavelengths of an AM0 spectrum, while the bottom cell absorbs the longer wavelengths, and the middle cell the intermediate wavelengths. Since the junctions are in series, the photocurrent in each junction is the same under power-generating conditions. The design of a triple-junction cell requires optimal junctions to convert the largest fraction of the AM0 spectrum into electrical energy. If the cell design is not optimal, then one of the junctions may limit the photocurrent, and carrier recombination in the other two junction will result in lower cell efficiency. The structure of the quantum efficiency of a triple-junction cell measured under AM0 D.C. light bias is useful in evaluating the design of the cell. If the measured QE resembles one of the curves in Figure 7, the results will suggest cell performance is limited by the junction which corresponds to the curve.

AM0 LIGHT-BIAS TRIPLE-JUNCTION QUANTUM EFFICIENCY RESULTS

The quantum efficieny of triple-juunction a-Si:H alloy solar cells were measured using a D.C. light-bias beam produced by the solar simulator adjusted to produce the spectral irradiance shown in Figure 3. The measurements were carried out with the cells under short-circuit current conditions. The results of measurements are shown in Figure 9. The peak value of QE is at 460 nm with a value of about 0.40. The curve in Figure 9 has approximately the same shape as the curve in Figure 7 for the top-junction of the cell. Figure 7 shows the peak value is 0.54 at 440 nm for the top junction of the cell measured. The results suggest the performance of the triple-junction cell under AM0 light bias is limited by the top junction. QE of three triple-junction cells were measured; the results of the measurements were convoluted with the solar simulator spectral irradiance using Equation 1 in order to obtain a calculated value for the short-circuit current. The results of the calculations are shown in Table II. Isc(calc) is within about 1% of Isc(meas) for the three cells. The calculations confirm the validity of the D.C. light-bias technique for determining QE of triple-junction cells.

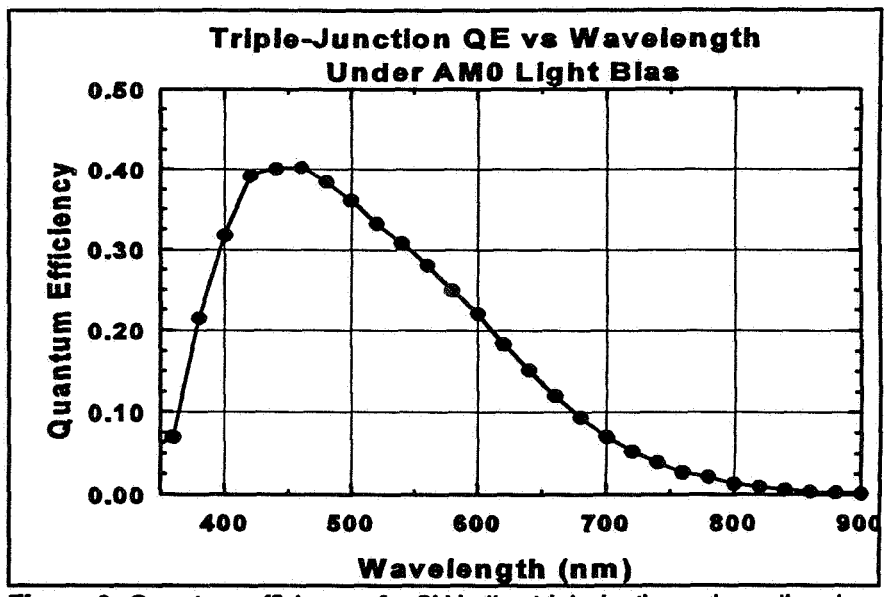

Figure 9: Quantum efficiency of a-Si:H alloy triple-juction solar cell under AM0 light bias.

Table II

Cell	Isc(meas) (mA)	Isc(calc) (ma)	ΔIsc/ Isc (%)
ST05	2.338	2.361	1.0%
ST17	2.386	2.395	0.4%
ST38	2.253	2.279	1.1%

The role of forward bias on QE of a triple-junction solar cells under AM0 D.C. light bias was investigated. A cell was maintained at 24 °C and QE measured with forward biases ranging between 0 and 1.82 V. The voltage at the

maximum-power point was about 1.7 V and the open-circuit voltage was about 2.2 V. Forward biases of 0, 0.62, 1.02, 1.42, 1.62 and 1.82 V were used. The results of the measurements are shown in Figure 10. Both the wavelength corresponding to the QE peak value and the peak value of QE are strongly influenced by the forward-bias voltage. The peak value of QE decreases from 0.40 to 0.08 as the forward bias increases from 0 to 1.82 V; for the same increases in the forward bias, the wavelength for the peak QE value increases from 460 to 600 nm. The measurements show QE under short-circuit conditions is considerably different than QE measured near the maximum-power point. While the short-circuit measurements suggest the performance of the cell is limited by the top junction, the measurements near the maximum-power point suggest both the top and middle junctions are limiting the operation of the cell.

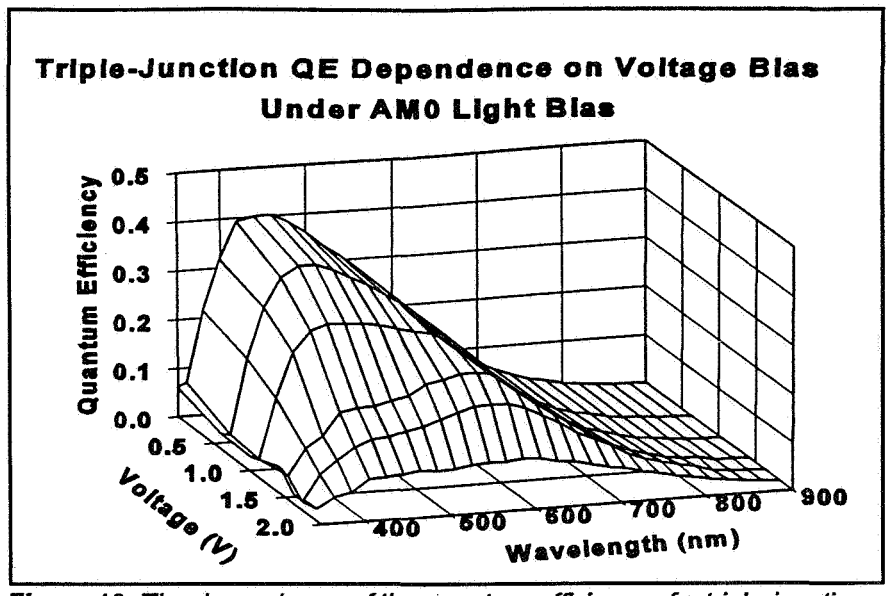

Figure 10: The dependence of the quantum efficiency of a triple-junction a-Si:H alloy solar cell on forward-bias voltage for AM0 light bias.

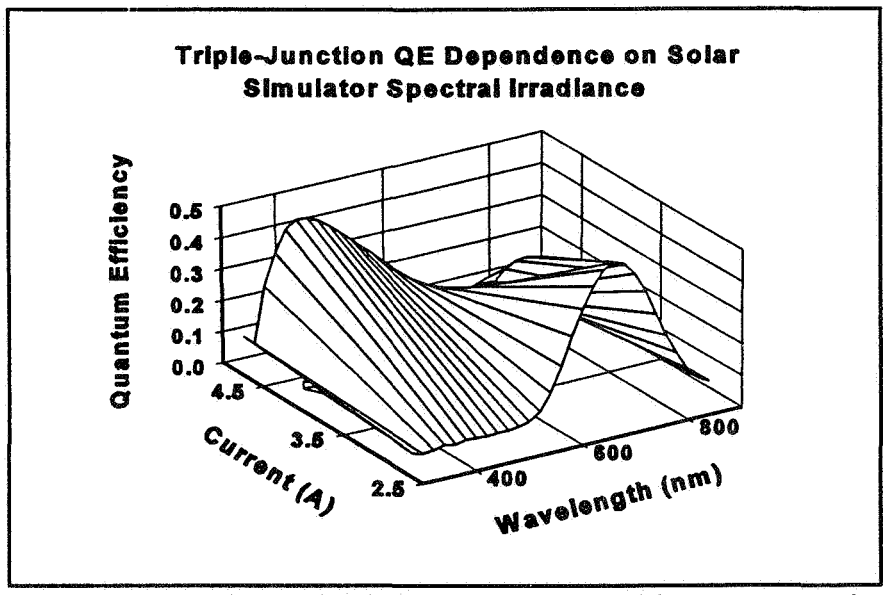

Figure 11: Dependence of triple-junction quantum efficiency on spectral irradiance of solar simulator. The spectral irradiance of the solar simulator was varied by changing the filament current in the tungsten-halide lamp.

The response of the triple-junction cell was further tested by qualitatively varying the spectral irradiance of the solar simulator by changing the current in the tungsten-halogen lamp. The lamp current was varied from 5.0 to 2.9 A; 5.0 A is the current which produced the fit to WRL AM0 shown in Figure 3. As the lamp current was decreased, the spectral irradiance beyond 750 nm decreased. Figure 11 shows the behavior of QE. The quantum efficiency with a lamp current of 5.0 A is the same as the values plotted in Figure 9. The QE curve with a lamp current of 2.9 peaks at 720 nm and has a value of 0.47; it is similar to the curve produced by the bottom junction shown in Figure 7. Thus as expected from the changes in the spectral irradiance produced by reducing the current in the tungsten-halogen lamp, the cell current is limited by the top junction when the lamp current is 5.0 A; the current in the bottom junction limits the cell current when the lamp current is 2.9 A.

The investigations of QE measured under AM0 light bias conditions reported in this section are preliminary, however, the results show agreement at the 1% level between measured short-circuit currents and currents calculated from measured cell quantum efficiencies and solar simulator spectral irradiances. Studies need to be done to determine the specifications of both the spectral irradiance and radiance of AM0 solar simulators to be used in the characterization of multi-junction cells. The accuracies will depend, among other things, on the number of junctions in the multi-junction cells and the optoelectronic properties of each of the junctions. The work to determine the

specifications for AM0 solar simulators can be carried out using small area cells, i.e., cells of the order of 1.0 cm^2 in area. While device simulation studies are useful for designing cell structures and defining the optoelectronic of each junction, laboratory characterization of cells should be carried out both to facilitate solar cell development and optimize the limited resources available for space testing.

SUMMARY

An integrated system was described which consists of a spectral radiometer and dual-source solar simulator, and personal computer based current-voltage and quantum efficiency equipment. The spectral radiometer was calibrated with a tungsten-halogen standard lamp. The quantum efficiency apparatus employed a calibrated reference detector which was used in measuring the absolute external quantum efficiency of triple-junction a-Si:H ally solar cells. The calibrations of the lamp and photodiode, as well as the source measurement unit used to measure cell currents were based on NIST scales. Quantum efficiencies were measured using both the spectral-light bias and AM0 light-bias techniques. Quantum efficiencies measured with the AM0 light-bias technique were shown to be dependent on forward-bias voltage and the spectral irradiance of the AM0 light-bias beam. Measured spectral irradiances and quantum efficiencies were convoluted to calculate cell short-circuit cell currents. Calculated currents compared with measured short-circuit currents at the 1% level .

REFERENCES

* Appreciation is expressed to Kenneth R. Lord II, Michael R. Walters and Fazal UrRahman Syed for their contributions to this work.

1. Joseph Burdick and Troy Glatfelter, Solar Cells **18** (1986) page 301.
2. M. Bennett and R. Podlesny Proceedings of the 21st IEEE Photovoltaic Specialists Conference (1990) page 1438.
3. Kenneth R. Lord II, Michael R. Walters and James R. Woodyard, Proceedings of the 23st IEEE Photovoltaic Specialists Conference (1993) page 1448.